Structural, Electronic and Magnetic Properties of Co$_n$O (n = 2～10) Clusters: A Density Functional Study

BAI Xi(白熙)[1,2];LIANG Rui-Rui(梁瑞瑞)[1];LV Jin(吕瑾)[1]

[1] *School of Chemistry and Material Science, Shanxi Normal University, Linfen* 041004, *China*;[2]

Pharmaceutical Department, Changzhi Medical College, Changzhi 046000, *China*

ABSTRACT The structural, electronic, and magnetic properties of Co$_n$O (n = 2～10) clusters have been systematically investigated within the framework of the generalized gradient approximation density functional theory. The results indicate that the O atom occupies the surface-capped position on Co$_n$O (n = 2～10) clusters. The stabilities of the host clusters are improved by adding one O atom. Maximum peaks of the second-order difference energy of the ground-state Co$_n$O clusters are found at n = 3, 6 and 8, indicating higher stability than their neighboring clusters. Compared with corresponding pure Co$_n$ clusters, the O-doped cobalt clusters have larger gaps between the HOMO and LUMO energy levels, indicating their higher chemical stabilities. In addition, the doping of O atom exhibits different influence on the magnetism of the clusters. This is also further investigated by the local magnetic moment, deformation charge density and partial local density of states analysis.

1 INTRODUCTION

Transition metal oxide clusters are widely used in high temperature chemistry, materials

science, microelectronics and nanotechnology areas, and have attracted extensive theoretical and experimental attention in the past ten years. For example, Clemmer *et al.*[1] reported experimental measurement of Sc–O bond energies and ionization potentials of ScO_2 using guided ion beam reactions between ScO^+ and NO_2. Wang *et al.*[2] have calculated the structural and magnetic properties of small transition metal oxide clusters TM_nO_m (TM = Sc, Ti, V, Cr and Mn; $n = 1, 2$; $m = 1 \sim 6$) by using *ab initio* density functional theory approach, and revealed that the geometries of clusters are closely correlated with the ratios of TM to O and the number of valence electrons of the TM atoms. Yang *et al.*[3, 4] studied the structural and electronic properties of La_nO ($n = 2 \sim 12$) clusters using the density functional theory (DFT), and found the doping of O atom prefers to stay outside the cluster, and can greatly improve the stability of small La_n clusters. In addition, the structures, electronic, and magnetic properties of transition metal (M = Cr, Mn, Fe, and Ni) oxide clusters and their anions and cations have been studied largely[5-12]. Gutsev G. L. *et al.*[13] studied the polarizability per atom of the MO monomers (M = Fe, Co, and Ni), and found that the doping resulted in a steep decrease of polarizability as compared to the atomic values. However, it is obvious that the existing theoretical study on Co_nO clusters is not sufficient, and that the detailed structural and electronic properties of the large size of Co_nO ($n \geqslant 5$) clusters are still unclear. Therefore, it is desirable to extend the study of Co_nO clusters to larger size so as to glean a comprehensive understanding of their exotic physical and chemical properties. We hope that our work can provide powerful guidelines for the corresponding experiments and promote the functional design of the clusters cohesive material. In the past decades, on the experimental side, the mass selected cobalt oxide cluster anions $Co_nO_m^-$ ($n = 5 \sim 21$, $m = 0 \sim 2$) are studied by using photodetachment photoelectron spectroscopy (PES), indicating that O atom causes a minor influence on the electronic structures[14]. Jacobson and Freiser[15] have performed Fourier transform mass spectrometry investigation on the reaction of cationic Co dimers and trimers with O_2. This was followed by a kinetic study of the reaction of small Co_n^+ clusters ($n = 2 \sim 9$) with O_2. On the theoretical side, Kosuke *et al.*[16] reported the results of structures of cobalt oxide cluster cations $Co_mO_n^+$ by ion mobility spectrometry (IMS), combined with the theoretical calculation in order to verify the structures of the clusters, and concluded that $(CoO)_{3-5}^+$ ions are

monocyclic-ring structures and $(CoO)_{6,7}{}^+$ has compact tower structures. Therefore, structural transition from the ring to compact structures occurs at $(CoO)_6{}^+$. The ground states of CoO_n ($n = 1\sim4$) and their anions $[CoO_n]^-$ were studied by density functional theory, with the BLYP exchange-correlation functional[17]. However, the researches on single O atom doped cobalt clusters are seldom investigated except Liu *et al.*[18] who study the structure and magnetic properties of the small-sized Co_nO ($n = 1\sim5$) clusters by using the density functional approach.

As far as we know, there is no systematical first principle calculation on the large size of Co_nO ($n = 2\sim10$) clusters. Our work aims to make clear how the O atom binds with the Co_n ($n = 2\sim10$) clusters by theoretical calculation with density functional theory method, and try to explore how the stability changes after O atom's doping with cobalt clusters, and how the magnetic properties of the host clusters are influenced by doping, finally to disclose the physical origin of the magnetic behavior of Co_nO clusters. We hope that our research work would provide a certain theoretical guidance for the practical application of cobalt oxide clusters assembling materials.

2 COMPUTATIONAL DETAILS

All calculations were performed at the DFT level with the $DMol^3$ package in the Materials Studio of Accelrys Inc[19]. The exchange-correlation interaction was treated within the GGA using PW91 function (GGA-PW91)[20]. The double numerical basis set augmented with *d*-polarization and *p*-polarization functions (DNP) was utilized. For the numerical integration, a fine quality mesh size was used, and the real space cutoff of the atomic orbital was set at 5.5 Å. The convergence criteria for structure optimization and energy calculations were set to fine with the tolerance for density convergence in SCF, energy, gradient and displacement 1×10^{-6} eV/Å, 1.0×10^{-5} a.u, 0.002 Hartree/Å and 0.005 Å, respectively. In geometry optimization procedure, we considered a number of initial structures including linear chains, planar and three-dimensional structures in this work to maximize our chance to find the ground state configurations of the alloy clusters. Meanwhile, we also look over other structures of La_nO, Sc_nO_m, Y_nO, Mn_nO, Nb_nO,

Co$_n$Rh, Co$_n$Mn, Co$_n$V and Co$_n$Fe[5, 21-28] clusters. In addition, owing to the spin polarization, all optimized geometry was optimized again at various possible spin multiplicities. Consequently, the number of possible initial isomers increased very rapidly with the size increase of clusters. The calculations are implemented until the minimum energy is reached. We confirm the stability of the lowest-energy structures as minima of the potential energy surface by considering no imaginary frequency.

To check the validity of the computational method in our work, we first perform the calculation on the Co$_2$ and CoO dimers using PW91, PBE and BLYP, respectively. As listed in Table 1, we choose the PW91 method finally because the results are consistent with previous theoretical and experimental data well, and these data are sufficient to show that it is effective and reliable to study Co$_n$O (n = 2~10) clusters with this method.

3   RESULTS AND DISCUSSION

3. 1   Geometrical structures of the Co$_n$O (n = 2~10) clusters

The low-lying geometries, symmetries, magnetic moment and energy relative (ΔE) of Co$_n$O (n = 2~10) clusters are shown in Figs. 1 and 2. The lowest energy structures of pure Co$_n$ clusters are also included for comparison. The lowest frequencies of Co$_n$ and Co$_n$O clusters are listed in Table 2.

For Co$_n$O clusters, a number of different stable configurations for each size cluster are found, but only three of them are shown in this paper. In the case of Co$_2$O cluster, the lowest-energy structure is an isosceles triangle (C_{2v}) with the O atom located at the apex. It has a total magnetic moment of 4 μ_B, which is consistent with previous theoretical calculation results exactly[19]. A less stable structure with 0.106 eV higher energy than the most stable one has more relaxed Co–Co and Co–O bonds to bring with a higher magnetic moment of 6 μ_B.

The most stable Co$_3$O cluster adopts a planar structure (C_{2v}) with 7 μ_B of total magnetic moment. Its metastable structure (3 μ_B), which shares the same geometric structure with the lowest-energy of Co$_3$O, is energetically less favorable than the most stable one by just 0.022 eV,

so they are two energetically degenerate states and magnetic bistable states. The third stable isomer is a tetrahedron (C_s) which is different from the ground state and metastable state totally. It is 5 μ_B in magnetic moment and 0.107 eV less stable in energy than the lowest energy structure.

A triangular bipyramid (8 μ_B) with the O atom located at the apex is found to be the most stable structure of Co_4O with C_s symmetry, which is in good agreement with the previous theoretical results[19]. In comparison, the second lowest-energy structure has similar geometry with the C_{3v} symmetry and lies 0.021 eV higher in energy with respect to the ground state. The next low-lying energy isomer (C_{2v}), which is energetically less stable than the most stable structure by 0.034 eV, exhibits double coordinating of O atom to the tetrahedron.

For the Co_5O cluster, we considered a lot of initial geometries including capped triangular bipyramid, octahedron and pentagonal pyramid. The lowest-energy structure is a capped triangular bipyramid (C_s) with an 11 μ_B of total magnetic moment, in which the O atom is located at the capped position. The second stable isomer (9 μ_B), which shares the same geometric structure and symmetry, is just 0.003 eV higher in energy than the lowest-energy structure. By contrast, the other stable isomer at a higher energy (0.012 eV) is different from the first two because the O atom tends to bind preferably to the bridge site of the Co_5O cluster.

Co_6O cluster (14 μ_B) adopts an O-capped octahedron structure with C_{3v} symmetry. In the metastable structure, the O atom coordinates with two connecting Co atoms and is coplanar with four Co atoms of the octahedron. The other low-lying structure (C_s) with 0.029 eV higher in energy shares the same configuration with the ground state, while has a smaller total magnetic moment of 12 μ_B which maybe results from the decrease in average bond length.

The ground-state structure of Co_7O (15 μ_B) is a bi-capped octahedron with C_s symmetry, in which the O atom is located at the capped position. The next two low-lying states have the same structure (C_{2v}) in which atom O lays coplanarly with the 5-membered ring of the hexagonal bipyramid. With total magnetic moments of 13 and 15 μ_B, their energies are higher than the ground-state structures by 0.044 and 0.051 eV, respectively.

The lowest-energy structure of Co_8O cluster can be viewed as a tricapped octahedron (C_s) with an 18 μ_B of total magnetic moment and the O atom is capped on the Co_8 ground-state geometry. The metastable state is a bicapped pentagonal bipyramid (C_{2v}) where O atom lies in the

middle plane and is opposite to the bicapped position. Its energy is 0.021 eV higher than the lowest energy structure. A side-capped tetrahedral prism geometrical isomer (C_s) with the O atom located at the capped position, which shares similar total magnetism with the ground state and the metastable state, is considered to be the next stable structure at a slightly higher energy (0.027 eV).

In terms of Co_9O, three low-lying structures are similar, which are all the bi-capped tetragonal antiprisms. The difference lies in the way how to cap. For the ground state structure (19 μ_B) with C_{4v} symmetry, the bi-capped atoms locate oppositely. While the metastable state and the third state are the same completely on structure (C_{3v}), in which the O impurity occupies an anterior capped position of pure Co_9 with notable instability (0.003 and 0.016 eV, respectively).

In the case of $Co_{10}O$, the structure is different from the Co_{10} cluster, which tends to form large layered structure of Co clusters. In addition, three low-lying structures have the same configuration and symmetry. The metastable state (18 μ_B) and the third state (14 μ_B) are higher in energy than the ground-state structure (20 μ_B) by 0.027 and 0.0055 eV, respectively.

From the above analysis, geometry optimizations reveal that O atom tends to bind preferably to the bridge site of the Co_2O and Co_3O clusters. About geometries of Co_nO (n = 5, 6, 7, and 8) clusters, we can see that O adds to bind preferably to three coordination sites with the ground state geometries of Co_n (n = 5, 6, 7, and 8), forming surface-capped structures. Although O atom also binds with three Co atoms in clusters of Co_4O and $Co_{10}O$, the way in which O atom binds is different. Their structures are based on the Co atoms rearrangement instead of the original ground-state structure of pure cobalt clusters. Additionally, for Co_9O, O binds to Co atom on the square edge in the most stable geometry. In a word, the results indicate that the O atom occupies the surface-capped position on Co_n (n =2～10) clusters. Meanwhile, we also found that a number of similar low energy isomers exist as the low-lying structures of the Co_nO (n = 2～10) clusters.

3. 2 Stabilities and electronic properties

To investigate the influence of doping of O on the stability of cluster, we computed and compared the average binding energies per atom of the lowest energy structures of Co_nO clusters and Co_n clusters (Fig. 3). The atomic average binding energy E_b (n) can be expressed by the following formulas:

$$E_b(Co_nO) = [nE(Co) + E(O) − E(Co_nO)]/(n + 1) \qquad (1)$$

$$E_b(Co_n) = [nE(Co) − E(Co_n)]/n \qquad (2)$$

where E is the total energy of the respective atom or cluster. n corresponds to the number of Co atoms in clusters. From Fig. 3, we can see that the average binding energies of Co_nO clusters are larger than those of Co_n clusters, indicating that the doping with O improves the stability of the main cluster. Moreover, the average binding energies of Co_nO clusters are increasing with the size, which indicates that these clusters can continuously gain energy during their growth. Specifically, in the initial stage ($n = 1\sim7$), E_b increases rapidly, while n goes from 7 to 10, the E_b exhibits obvious convergence trend. The change trend of E_b for pure Co clusters matches with the previous theoretical results well[26, 28, 29].

In cluster physics, the second-order difference of cluster energies is another important quality that can reflect the relative stability of clusters. The second-order difference energy $\Delta_2E(n)$ is also calculated using the following formulas below and plotted in Fig. 3:

$$\Delta_2E(Co_n) = E(Co_{n+1}) + E(Co_{n-1}) − 2E(Co_n) \qquad (3)$$

$$\Delta_2E(Co_nO) = E(Co_{n+1}O) + E(Co_{n-1}O) − 2E(Co_nO) \qquad (4)$$

where E is the total energy of cluster. As shown in Fig. 3, the $\Delta_2E(n)$ exhibits an obvious even-odd oscillatory behavior for Co_n clusters, indicating that the Co_n clusters with even number of atoms are more stable than their neighboring sizes. A similar trend is observed in Co_nO clusters except for Co_3O. The local peaks are found at $n = 3$, 6 and 8, which indicates that these clusters are relatively more stable than their neighboring clusters. Meanwhile, local minimum peaks appear at $n = 5$, 7 and 9 identically. Overall, the doping of O atom does not influence the change trend of the stability of clusters.

In addition, the HOMO-LUMO gap is a characteristic quality of electronic structure and stability in clusters and is commonly used to measure the ability for clusters to undergo activated chemical reactions with small molecules. As shown in Table 2, the HOMO-LUMO gaps of Co_nO are usually larger than those of Co_n clusters except for $n = 8$, suggesting their high chemical inertness of the doped Co_nO clusters. The reason for the larger E_{gap} is that the O atom's doping makes the Co–Co interaction weak in clusters, leading to the large E_{gap}[34]. That is consistent with

the trend of the binding energies. Moreover, noticeable peaks of E_{gap} are found at $n = 3$, 6 and 10, indicating that these clusters must be more stable than the neighboring sizes. However, the stabilities of clusters for $n = 5$ and 8 are low.

To understand the differences of HOMO-LUMO gaps between Co_n and Co_nO clusters, the pictorial representation of molecular orbitals for $n = 2$, 4, 6, and 8 is used and plotted in Fig. 4. By this way, the types of orbitals involved in the bond formation can be seen clearly. For Co_2, the HOMO consists of an anti-bonding d_{z^2} orbital along the bond axis, while the LUMO is also noticed to be an anti-bonding but from s orbital. With the doping of O atom, an obvious π bond formed by d_{z^2} orbitals of Co atoms accounts for the HOMO of Co_2O cluster, which results in energy reduction dramatically. In the LUMO of Co_2O cluster, the d_{z^2} orbitals bond weakly with p orbital of O atom but still an anti-bonding orbital. Compared with Co_2, the bonding in Co_2O reduces the energies of HOMO largely and LUMO slightly, so it is responsible for the largest gap difference among all the pairs (Co_n/Co_nO). The HOMO diagram of Co_4 is noticed to a strong bond between $d_{x^2-y^2}$ from para-Co atoms and s orbitals from the other two, exhibiting a distinct d-p hybridization characteristic. While, the LUMO locates 0.507 eV higher in energy and consists of a non-bonding from four d orbitals (d_{yz} and d_{xz}). When doped with one O atom, it exhibits nonbonding overlap in HOMO which is higher in energy than that of Co_4. The LUMO of Co_4O shows nonbonding as well as anti-bonding overlaps. As the cluster size n goes to 6, the HOMO consists of six d_{xy} being nonbonding and σ bond is observed in LUMO, which contributes a small HOMO-LUMO gap. After doping with an O atom, a large π overlap is induced in HOMO and an in-plane π bond in LUMO. Meanwhile, the LUMO also has a non-bonding perpendicular to the π bond, resulting in a much lower HOMO and a higher LUMO. Both the HOMO and LUMO of Co_8 are mainly composed of nonbonding overlaps of d orbitals, while some obvious sideway overlaps between s, p and d orbitals appearing in HOMO, forming d-s, d-p and d-d delocalized σ bonds. Moreover, there is an obvious π bond in the LUMO of Co_8O cluster. Therefore, the enhancement of bonding causes an overall reduction in energy level and a tiny decrease in gap compared to Co_8 cluster.

We also perform Mulliken population analysis for the lowest-energy structures, and the atomic charges of O atom are presented in Table 2. It shows clearly that all of the O atoms are negatively charged. There is an obvious charge transfer from Co to O, indicating that the O atom is a Mulliken charge receiver. Furthermore, the charge transfer means the presence of ionic bonds between Co and O in Co_nO clusters. It is an important reason for the higher stability of the doped Co_nO clusters[35].

In order to understand the charge distribution between Co and O atoms of the doped clusters, we analyzed the charge difference density of Co_3O and Co_6O clusters. The difference charge density is defined as the difference between the total charge density of the cluster and a superposition of atomic charge densities with the same spatial coordinates in the cluster. As is shown in Fig. 5, the red color means charge accumulation, while the blue represents charge depletion. Strong charge accumulation is observed around the O atom both in Co_3O and Co_6O, while the depletion of charge is found from vacuum to Co site. Significantly, the electron accumulation is highly localized, signifying the characteristic of ionic bond between O and its neighboring Co atoms. Additionally, we can conclude that the extent of charge accumulation on O atom is greater in Co_6O than in Co_3O.

3.3 Magnetic properties

Following, we will focus on the magnetic properties of Co_nO ($n = 2\sim10$) clusters. The total magnetic moment of the ground-state Co_nO ($n = 2\sim10$) clusters has been calculated and the results are presented in Figs. 1 and 2. For comparison, the values of pure cobalt clusters are also plotted. Clearly, the total magnetic moments of Co_nO clusters increase with the size, which shows a similar trend with Co_n clusters. For $n = 2, 3, 6, 7$ and 10, the total magnetic moments of clusters even remain constant after doping with the O impurity, and those of the Co_n ($n = 4, 5$) clusters decrease while the values increase for $n = 8$ and 9. Interestingly, whether the moment increases or decreases, it keeps a difference of 2 μ_B. The magnetic behavior of Co_nO ($n = 1, 3, 5$) clusters is similar to that of the previous theoretical work[18].

In order to explore the magnetic origin further, we selected the ground state Co_nO ($n = 5$, 7, 9) clusters as representatives to discuss the influence of the doping of O atom on local

magnetic moment of the main clusters (Fig. 6). For comparison, the local magnetic moment per atom of corresponding pure Co_n clusters is shown in Fig. 6. As is evident from the figure, the magnetic moments of the Co_nO clusters are chiefly derived from the Co atom and the contribution of O atom is very small. Additionally, the magnetic moment reduction or enhancement upon doping stems from the reduced or increased local magnetic moments on the Co atoms. For instance, as for the Co_5O cluster, the local magnetic moment of Co atom is reduced because of the doping of O atom, resulting in decrease on the total spin moment in contrast with the corresponding pure Co_5 cluster. In the case of $n = 9$, accompanying the enhanced local magnetic moments on Co in the doped cluster, the total magnetic moment increases. For the cases of $n = 7$, the O's doping redistributes the spin moment on the Co atoms and the local moments decrease for the Co atoms near O and increase for those at a distance overall, thus the total magnetic moments of the clusters remain unaltered before and after loading O. A similar phenomenon also appears in previous study on the magnetism of atomic oxygen adsorbed Sc_n ($n = 2\sim14$) clusters[36].

To further understand the magnetic mechanism of Co_nO ($n = 1\sim9$) clusters, we provide the partial (PDOS) and local (LDOS) contribution of different orbital components of Co_5O, Co_7O and Co_9O clusters as representatives. As is evident from Fig. 7, firstly, we note that the magnetism of Co_nO is mainly from the contribution of Co atoms in which their electronic states below Fermi level come primarily from d electron state and the contributions from s and p electron states are very small. For the O atom, below the Fermi level, the integral area of spin-up p electrons is nearly equal to the spin-down p electrons in LDOS, indicating that the doping of O atom can hardly affect the magnetism of clusters, which coincided with the above analysis about local magnetic moment of clusters. In addition, between the Fermi level of –4 and –6 eV, there is a clear indication of hybridization between O $2p$ and Co $3d$, resulting in the rearrange of charge density and in turn influences the magnetic moment of cobalt clusters. Generally speaking, the relative shift between the spin-up and spin-down bands can indicate the degree of spin exchange splitting. Moreover, the greater spin exchange splitting, the larger spin polarization and magnetic moment of cluster[37]. As shown in Fig. 7, for Co_5O cluster, we find that the spin-up d electrons integral area of Co_5O/Co_5 is evidently smaller than that of the pure Co_5 cluster. Meanwhile, the d

electron peak of spin-down of Co_5O cluster is broadened around –5.5 eV below the Fermi level, which further counteracts the spin-up d electrons, indicating that the spin exchange splitting of DOS is decreased obviously. So, the total magnetic moment is decreased after O doping the pure Co_5 cluster. Compared with Co_7 cluster, there is no much change on spin exchange splitting of Co_7O/Co_7, and the differences of integral areas between spin-up and spin-down d electrons in pure Co_7 cluster and Co_7O/Co_7 are similar, so the total spin moment of Co_7O cluster remains unchanged. In addition, we find that the spin exchange splitting of Co_9O/Co_9 is obvious, and the integral area of spin-up d electrons is evidently larger than that of spin-down below the Fermi level in LDOS, resulting in the increasing magnetism of the doping-O cobalt clusters.

4 CONCLUSION

By using the first-principles DFT-GGA calculations, the geometries, stabilities, and magnetic properties of the O doped Co_n clusters have been systematically studied, with the results summarized as follows:

(1) In the most stable structures of Co_nO clusters, the O atom prefers to occupy the surface-capped position of Co_n ($n = 2\sim10$) clusters. Geometry optimizations reveal that O atom tends to bind the bridge site in the Co_2O and Co_3O clusters; the O atoms are capped by three coordination in Co_nO ($n = 5, 6, 7$ and 8) clusters; for Co_9O cluster, the O atom is capped by four coordination, in which the corresponding Co_n maintains its original ground state structure of pure cobalt cluster. In addition, by analyzing the most stable geometries of Co_4O and $Co_{10}O$ clusters, we also found that the O atom prefers to bind with Co atoms in a way of three-coordinate, but Co atoms appear obvious rearrangement, and the $Co_{10}O$ cluster exhibits a layer structure model.

(2) From the analysis of the second-order energy difference, we can conclude that Co_nO clusters at $n = 3, 6$, and 8 possess relatively higher stabilities than their neighbors, which means that the doping of O atom improves the stability of the Co_3O, Co_6O and Co_8O clusters.

(3) By analyzing the HOMO and LUMO of Co_n and Co_nO ($n = 2, 4, 6, 8$) clusters, we can

conclude that the gap is mainly determined by the bonding strength between atomic orbitals.

(4) Compared to those of pure cobalt clusters, the magnetism calculations show that the total magnetic moments for Co_nO clusters emerge different changing trends. Because of the hybridization between the $3d$ state of Co and the $2p$ state of doping-O, the local magnetic moments of Co atoms changed. However, the contribution of spin moments from O atom is negligible in Co_nO clusters. Thus, the magnetic moment reduction or enhancement by doping can be attributed to the decrease and increase of the local magnetic moments of the Co atoms.

REFERENCES

(1) Clemmer, D. E.; Dalleska, N. F.; Armentrout P. B. Gas-phase thermochemistry of the group 3 dioxides: ScO_2, YO_2 and LaO_2. *Chem. Phys. Lett.* **1992**, 190, 259−265.

(2) Wang, Y. B.; Gong, X. X.; Wang, J. L. Comparative DFT study of structure and magnetism of TM_nO_m (TM = Sc-Mn, $n = 1 \sim 2$, $m = 1 \sim 6$) clusters. *Phys. Chem. Chem. Phys.* **2010**, 12, 2471−2477.

(3) Xu, B. F.; Yang, C. L.; Wang, M. S.; Ma, X. G. The geometric structure and electronic properties of $Fe_3O_3^+$ clusters. *Physica B* **2011**, 406, 200−204.

(4) Logemann, R.; de Wijs, G. A.; Katsnelson, M. I.; Kirilyuk, A. Geometric, electronic, and magnetic structure of $Fe_xO_y^+$ clusters. *Phys. Rev. B* **2015**, 92, 144427.

(5) Reddy, B. V.; Khanna, S. N.; Ashman, C. Oscillatory magnetic coupling in Cr_2O_n ($n = 1 \sim 6$) clusters. *Phys. Rev. B* **2000**, 61, 5797−5801.

(6) Tono, K.; Terasaki, A.; Ohta, T.; Kondow, T. Chemically induced ferromagnetic spin coupling: electronic and geometric structures of chromium-oxide cluster anions $Cr_2O_n^-$ ($n = 1 \sim 3$) studied by photoelectron spectroscopy. *J. Chem. Phys.* **2003**, 119, 11221−11227.

(7) Veliah, S.; Xiang, K. H.; Pandey, R. J.; Recio, J. M.; Newsam, J. M. Density functional study of chromium oxide clusters: structures, bonding, vibrations, and stability. *J. Phys. Chem. B* **1998**, 102, 1126−1135.

(8) Wang, Q.; Sun, Q.; Sakurai, M.; Yu, J. Z.; Gu, B. L.; Sumiyama, K.; Kawazoe, Y. Geometry and electronic structure of magic iron oxide clusters. *Phys. Rev. B* **1999**, 59, 12672−12677.

(9) López, S.; Romero, A. H.; Mejía-López, J.; Mazo-Zuluaga, J.; Restrepo, J. Structure and electronic properties of iron oxide clusters: a first-principles study. *Phys. Rev. B* **2009**, 80, 085107− 085107.

(10) Knickelbein, M. B. Nickel clusters: the influence of adsorbates on magnetic moments. *J. Chem. Phys.* **2002**, 116, 9703−9711.

(11) Jones, N. O.; Khanna, S. N.; Baruah, T.; Pederson, M. R.; Zheng, W. J.; Nilles, J. M.; Bowen, K. H. Magnetic isomers and local moment distribution in Mn_5O and Mn_6O clusters. *Phys. Rev. B* **2004**, 70, 134422−134422.

(12) Williams, K. S.; Hooper, J. P.; Horn, J. M.; Lightstone, J. M.; Wang, H. P.; Ko, Y. J.; Bowen, K. H. Magnetic structure variation in manganese-oxide clusters. *J. Chem. Phys.* **2012**, 136, 134315−134315.

(13) Gutsev, G. L.; Belay, K. G.; Bozhenko, K. V.; Gutsev, L. G.; Ramachandran, B. R. A comparative study of small $3d$-metal oxide $(FeO)_n$, $(CoO)_n$, and $(NiO)_n$ clusters. *Phys. Chem. Chem. Phys.* **2016**, 18, 27858.

(14) Pramann, A.; Koyasu, K.; Nakajima, A. Photoelectron spectroscopy of cobalt oxide cluster anions. *J. Phys. Chem. A* **2002**, 106, 4891−4896.

(15) Jacobson, D. B.; Freiser, B. S. Transition-metal cluster ions in the gas phase. Oxide chemistry of dimeric and trimeric clusters containing iron and cobalt. *J. Am. Chem. Soc.* **1986**, 108, 27−30.

(16) Ota, K.; Koyasu, K.; Ohshimo, K.; Misaizu, F. Structures of cobalt oxide cluster cations studied by ion mobility mass spectrometry. *Chem. Phys. Lett.* **2013**, 588, 63−67.

(17) Uzunova, E. L.; Nikolov, G. S.; Mikosch, H. Electronic structure and vibrational modes of cobalt oxide clusters CoO_n ($n = 1 \sim 4$) and their monoanions. *J. Phys. Chem. A* **2002**, 106, 4104−4114.

(18) Liu, L.; Zhao, R. N.; Han, J. G.; Liu, F. Y.; Pan, G. Q.; Sheng, L. S. Does the incoming oxygen atom influence the geometries and the electronic and magnetic structures of Co_n clusters *J. Phys. Chem. A* **2008**, 113, 360−366.

(19) Delley, B. An all-electron numerical method for solving the local density functional for polyatomic molecules. *J. Chem. Phys.* **1990**, 92, 508−517.

(20) Perdew, J. P.; Burke, K.; Ernzerhof, M. Generalized gradient approximation made Simple. *Phys. Rev. Lett.* **1996**, 77, 3865−3868.

(21) Yang, Y.; Liu, H. T.; Zhang, P. Structural and electronic properties of Sc_nO_m ($n = 1 \sim 3$, $m = 1 \sim 2n$) clusters: theoretical study using screened hybrid density functional theory. *Phys. Rev. B* **2011**, 84, 205430.

(22) Yang, Z.; Xiong, S. J. Structural, electronic, and magnetic properties of Y_nO ($n = 2 \sim 14$) clusters: density functional study. *J. Chem. Phys.* **2008**, 129, 124308.

(23) Han, M. J.; Ozaki, T.; Yu, J. Electronic structure and magnetic properties of small manganese oxide clusters. *J. Chem. Phys.* **2005**, 123, 034306.

(24) Wang, H. Q.; Li, H. F. Density functional study on structures, stabilities, electronic and magnetic properties of Nb_nO ($n = 3 \sim 10$) clusters. *Comput. Theor. Chem.* **2013**, 1006, 70−75.

(25) Shen, N. F.; Wang, J. L.; Zhu, L. Y. *Ab initio* study of magnetic properties of bimetallic $Co_{n-1}Mn$ and $Co_{n-1}V$ clusters. *Chem. Phys. Lett.* **2008**, 467, 114−119.

(26) Datta, S.; Kabir, M.; Saha-Dasgupta, T.; Mookerjee, A. Structure, reactivity, and electronic properties of V-doped Co clusters. *Phys. Rev. B* **2009**, 80, 085418.

(27) Zhang, Y.; Duan, Y. N.; Zhang, J. M.; Xu, K. W. Structures, stabilities and magnetic properties of $FeCo_{n-1}$ ($n \leqslant 16$) clusters. *J. Magn. Magn. Mater.* **2011**, 323, 842−848.

(28) Lv, J.; Bai, X.; Jia, J. F.; Xu, X. H.; Wu, H. S. Structural, electronic and magnetic properties of Co$_n$Rh (n = 1∼8) clusters from density functional calculations. *Phys. B: Condensed Matt.* **2012**, 407, 14−21.

(29) Ma, Q. M.; Xie, Z.; Wang, J.; Liu, Y.; Li, Y. C. Structures, stabilities and magnetic properties of small Co clusters. *Phys. Lett. A* **2006**, 358, 289−296.

(30) Sebetci, A. Cobalt clusters (Co$_n$, n = 2∼6) and their anions. *Chem. Phys.* **2008**, 354, 196−201.

(31) Kant, A.; Strauss, B. Dissociation energies of diatomic molecules of the transition elements. II: titanium, chromium, manganese, and cobalt. *J. Chem. Phys.* **1964**, 41, 3806−3808.

(32) Chuang, Y. Y.; Schmid, R.; Chang, Y. A. Magnetic contributions to the thermodynamic functions of pure Ni, Co, and Fe. *Met. Trans. A* **1985**, 16, 153−165.

(33) Pedley, J. B.; Marshall, E. M. Thermochemical data for gaseous monoxides. *J. Phys. Chem. Ref. Data* **1983**, 12, 967−1031.

(34) Feng, R. J.; Xu, X. H.; Wu, H. S. Electronic structure and magnetism in (CoPt)$_n$ (n ⩽ 5) clusters. *J. Magn. Magn. Mater.* **2007**, 308, 131−136.

(35) Zhao, H. Y.; Wang, J.; Liu, Y.; Li, Y. C. The effects of nitrogen on the configurations and magnetic moments of small iron, cobalt and nickel clusters. *Eur. Phys. J. Appl. Phys*. **2009**, 48, 30601.

(36) Wang, J. L.; Wang, Y. B.; Wu, G. F.; Zhang, X. Y.; Zhao, X. J. *Ab initio* study of the structure and magnetism of atomic oxygen adsorbed Sc$_n$ (n = 2∼14) clusters. *Phys. Chem. Chem. Phys.* **2009**, 11, 5980−5985.

(37) Zhang, G. W.; Feng, Y. P.; Ong, C. K. Local binding trend and local electronic structures of 4d transition metals. *Phys. Rev. B* **1996**, 54, 17208−17214.

Table 1. Calculated Bond Lengths and Binding Energy per Atom of the Co$_2$ and CoO Clusters Using Different Density Functional Theory Methods

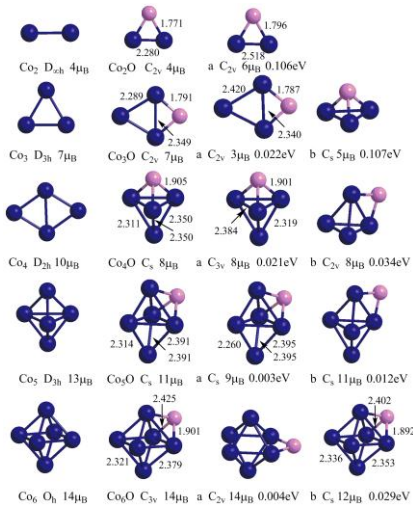| Methods	Co$_2$		CoO	
	R (Å)	E_b (eV/atom)	R (Å)	E_b (eV/atom)
PBE	2.139	2.791	1.642	3.453
PW91	2.134	2.851	1.642	3.489
BLYP	2.155	2.626	1.655	3.306
Theoretical	2.123/2.130[28, 29]	2.74[28]	1.595[17]	
Experimental	2.31[30]	1.72[30]	1.631[31]	3.94±0.14[32]

Fig. 1. Ground-state geometries of the corresponding bare Co$_n$ clusters and the lowest-energy structures and low-lying isomers of Co$_n$O (n = 2∼6) clusters. Distances are given in Å
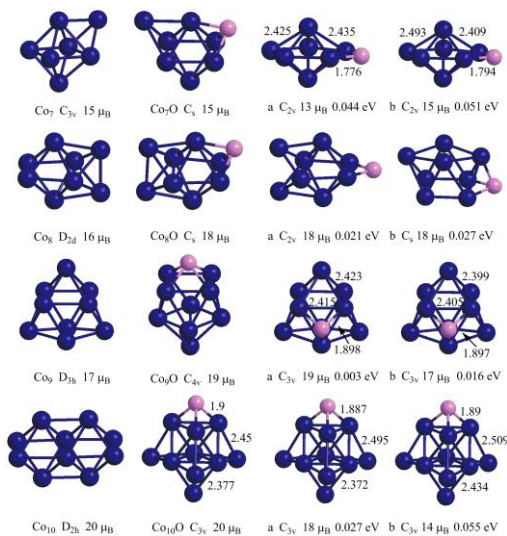
Fig. 2. The same as those in Fig. 1 but for *n* = 7, 8, 9 and 10. Distances are given in Å

Table 2. Frequencies (cm⁻¹), HOMO-LUMO Gaps (eV) and Total Spin Magnetic Moments (μ$_B$) of Co$_n$/Co$_n$O Clusters. The Charges (e) on O Atoms of Co$_n$O Clusters Are also Presented

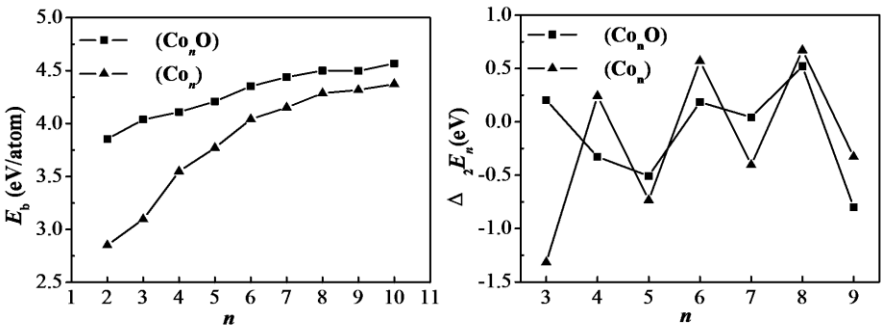| Cluster size (*n*)	Frequency	HOMO-LUMO gap	Charge
2	327.9/224.6	0.263/0.886	−0.681
3	257.7/43.9	0.632/0.946	−0.680
4	71.6/119.3	0.507/0.756	−0.693
5	86.5/42.5	0.353/0.590	−0.694
6	140.4/121.2	0.233/0.658	−0.695
7	69.8/76.6	0.353/0.642	−0.691
8	79.1/81.5	0.423/0.370	−0.689
9	85.4/42.7	0.198/0.389	−0.683
10	70.6/30.9	0.257/0.431	−0.692

Fig. 3. Average binding energies per atom and the second-order difference energies of the most stable structures of Co$_n$ and Co$_n$O clusters as a function of cluster size
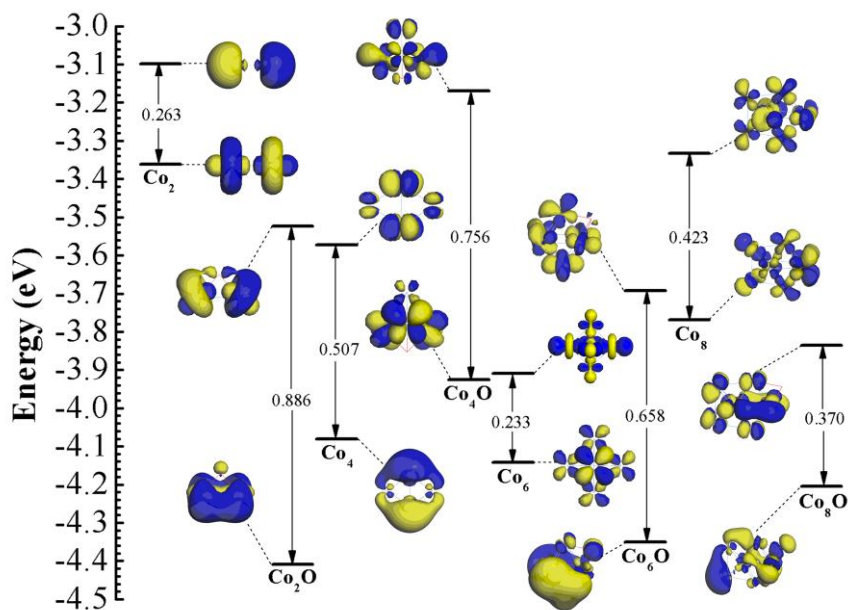
Fig. 4. 3*D* isosurface HOMO and LUMO diagrams of Co*n* and Co*n*O clusters (*n* = 2, 4, 6, 8)
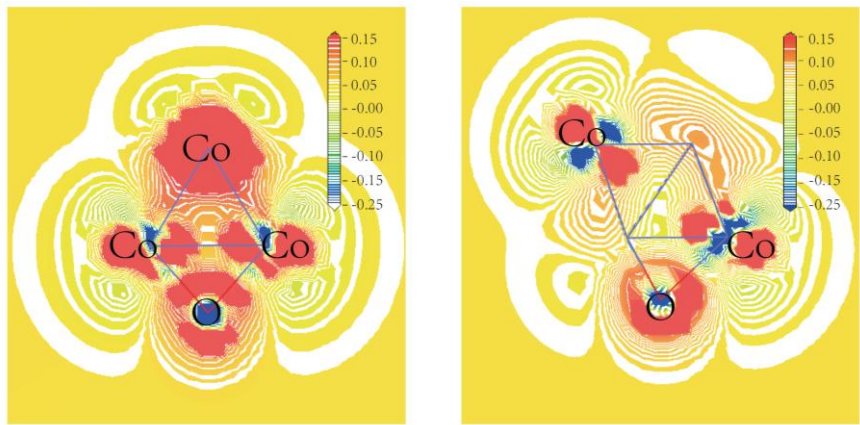

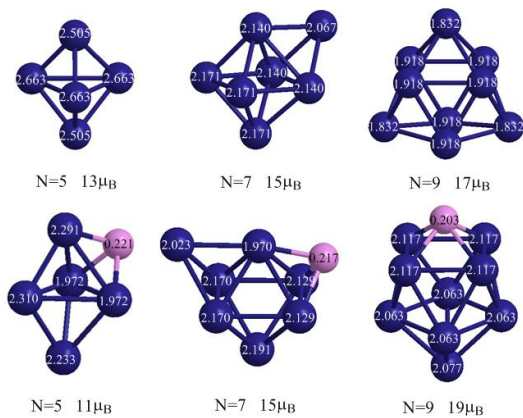**Fig. 5.** Calculated deformed charge density plots for Co₃O (left) and Co₆O (right)

Fig. 6. Local atomic magnetic moments on each atom of the lowest energy structures of Co*n*O (*n* = 5, 7, 9)
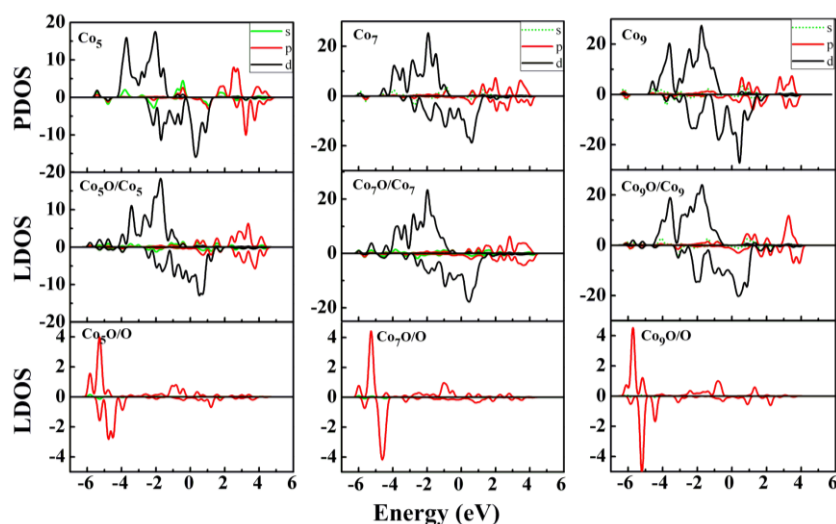
Fig. 7. Partial (PDOS) and local (LDOS) density of states of Co_n and Co_nO ($n = 5, 7, 9$) clusters. The broadening width parameter is chosen as 0.1 eV

Structural, Electronic and Magnetic Properties of

Co_nO ($n = 2\sim10$) Clusters: A Density Functional Study

BAI Xi(白熙)　　LIANG Rui-Rui(梁瑞瑞)　　LV Jin(吕瑾)

The structural, electronic, and magnetic properties of Co_nO ($n = 2\sim10$) clusters have been systematically investigated by density functional theory. The results indicate that the O atom occupies the surface-capped position on Co_nO ($n = 2\sim10$) clusters. The doping of O atom on Co_n cluster improves the stability of the host cluster and Co_3O, Co_6O and Co_8O clusters exhibit higher stabilities than their neighboring clusters. The charge distribution between O and Co in Co_nO clusters shows that O atoms are of great ionic character. The magnetic moment reduction or enhancement by doping can be attributed to the decrease and increase of the local magnetic moments of the Co atoms. In other words, the doping-O atom almost has no effect on the total spin moment. The doping-O atoms contribute little to the total moments of Co_nO clusters, but O atoms induce different influences on the local magnetic moments of neighbor Co atoms, which finally change the total moments differently.